

A new antiproliferative noscapine analogue: chemical synthesis and biological evaluation

Peter E. Ghaly¹, Rabab M. Abou El-Magd^{2,4}, Cassandra D. M. Churchill¹, Jack A. Tuszynski^{2,3}, F. G. West¹

¹Department of Chemistry, University of Alberta, Edmonton, AB T6G 2G2, Canada

²Department of Oncology, University of Alberta, Edmonton, AB T6G 1Z2, Canada

³Department of Physics, University of Alberta, Edmonton, AB T6G 2E1, Canada

⁴Genetic Engineering and Biotechnology Institute, City of Scientific Research and Technological Application, New Borg El-Arab City, Alexandria, 21934, Egypt

Correspondence to: F. G. West, email: frederick.west@ualberta.ca
Jack A. Tuszynski, email: jackt@ualberta.ca

Keywords: noscapine, tubulin, microtubules, fluorescence quenching, docking

Received: October 28, 2015

Accepted: April 10, 2016

Published: May 26, 2016

ABSTRACT

Noscapine, a naturally occurring opium alkaloid, is a widely used antitussive medication. Noscapine has low toxicity and recently it was also found to possess cytotoxic activity which led to the development of many noscapine analogues. In this paper we report on the synthesis and testing of a novel noscapine analogue. Cytotoxicity was assessed by MTT colorimetric assay using SKBR-3 and paclitaxel-resistant SKBR-3 breast cancer cell lines using different concentrations for both noscapine and the novel compound. Microtubule polymerization assay was used to determine the effect of the new compound on microtubules. To compare the binding affinity of noscapine and the novel compound to tubulin, we have done a fluorescence quenching assay. Finally, in silico methods using docking calculations were used to illustrate the binding mode of the new compound to α,β -tubulin. Our cytotoxicity results show that the new compound is more cytotoxic than noscapine on both SKBR-3 cell lines. This was confirmed by the stronger binding affinity of the new compound, compared to noscapine, to tubulin. Surprisingly, our new compound was found to have strong microtubule-destabilizing properties, while noscapine is shown to slightly stabilize microtubules. Our calculation indicated that the new compound has more binding affinity to the colchicine-binding site than to the noscapine site. This novel compound has a more potent cytotoxic effect on cancer cell lines than its parent, noscapine, and hence should be of interest as a potential anti-cancer drug.

INTRODUCTION

Noscapine, a phthalide isoquinoline alkaloid, is a natural product that was first isolated and characterized in 1817 by Pierre-Jean Robiquet [1] from the opium poppy, *Papaver somniferum*. Unlike other opium alkaloids, noscapine is non-addictive, non-narcotic and non-analgesic. It is widely used in many countries as an antitussive (cough suppressant) agent and has a low toxicity profile [2]. In 1998, the Joshi group found that noscapine possesses anticancer activity due to its action on tubulin [3]. As a tubulin-binding agent, noscapine

has some pharmacological advantages. Noscapine was found to be effective in slowing tumour growth while having little toxicity in normal tissues [4], is effective in multidrug resistant cell lines [5], and has a favorable pharmacokinetic profile [6]. Noscapine is also known to trigger apoptosis in different cancer cell lines through the activation of different apoptotic pathways [7–10]. Over the last decade, many noscapine analogues have been synthesized and tested, showing anti-cancer activity superior to the parent noscapine. These analogues are synthesized by chemically modifying the parent noscapine molecule, while keeping the

scaffold intact. The first generation noscapinoids were generated by chemically modifying the isoquinoline and benzofuranone rings of noscapine. This includes the 9'-halogenated (chloro-, bromo- and iodo-noscapine) [11], 9'-amino [12], 9'-nitro [13] and the 9'-azido analogues [14]. The first generation also includes cyclic ether halogenated analogues [15]. O-alkylated and O-acylated analogues represent the second-generation noscapinoids that were generated by modifying the benzofuranone ring of noscapine [16]. Third-generation noscapinoids were synthesized by modifying the substituents coupled to the nitrogen of the isoquinoline ring (Figure 1) [17].

Noscapine binds to tubulin stoichiometrically [18] to induce a conformational change in the protein [3], as found for other anti-mitotic agents that target tubulin [19,20]. Noscapine is unique from other antimitotic agents since it has no significant effect on microtubule stabilization or destabilization [5], but instead alters the dynamic instability of microtubules by increasing the time spent in the pause phase [5]. Similar structural features between noscapine and colchicine, a known destabilizing agent [21], initially suggested these compounds may bind to the same site, although experiments found that noscapine does not compete with colchicine for binding to tubulin [3]. Interestingly, a small modification altering noscapine to 9-bromonoscapine results in a compound that disrupts colchicine binding [22], and slightly inhibits microtubule polymerization [23]. Therefore, understanding how noscapine and its analogues bind to and affect tubulin and microtubules has proven challenging without crystal structures or hydrogen-deuterium exchange mass spectrometry.

In 2011, using computational docking and molecular dynamics methods, noscapine was predicted to bind to a unique site on β -tubulin at the intradimer interface that is near the colchicine site, but does not interfere with colchicine binding [24]. This result was supported by competitive binding experiments showing

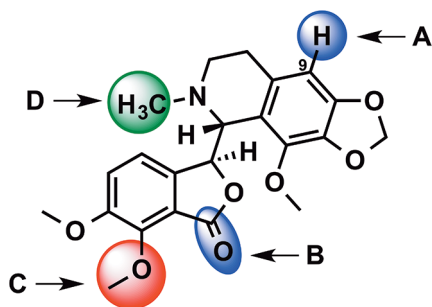


Figure 1: Structural modification of noscapine. A. and B. represent sites of modification of the first generation noscapinoids. Second and third generation noscapinoids were generated by modifications at sites C. and D. respectively.

a lack of competition between noscapine and colchicine [3]. Based on this newly identified binding site, a new library of noscapine analogues was proposed, which were computationally predicted to have higher affinity towards tubulin than noscapine [24]. These newly proposed analogues share a common scaffold within their structures. In our subsequent attempts to synthesize this common scaffold, we came across an interesting compound that showed promising anti-proliferative activity compared to noscapine.

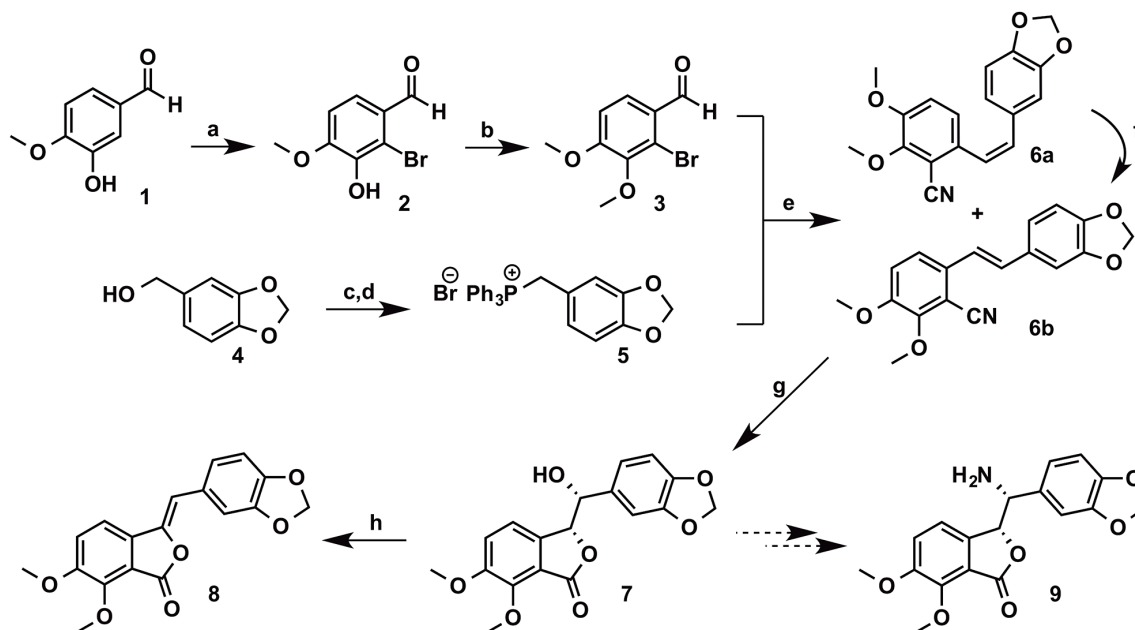
In this study, we report the effect of this novel compound 8, on SKBR-3 breast cancer cells, its affinity towards tubulin, as well as its effects on microtubule polymerization. We have also studied the binding of this compound to various sites on tubulin using *in silico* methods.

RESULTS

Synthetic pathway for the new compound (8)

Our synthesis (Scheme 1) began with the commercially available isovanillin 1. Regioselective bromination of 1 gave the 2-bromoisovanillin 2 [25] in 83% yield. This was followed by methylation of the phenolic hydroxyl group in 2 to give the 2-bromo-3,4-dimethoxybenzaldehyde 3 [26] in 76% yield. The phosphonium salt 5 was synthesized from the piperonyl alcohol 4 according to the literature procedure [27] in 93% overall yield. Compounds 3 and 5 were then coupled under Wittig reaction conditions to give inseparable *E/Z* olefin mixture, which was then treated with CuCN to afford a separable mixture of 6a/6b in 80% global yield with 60:40 ratio in favor of 6a [28]. The *Z*-isomer 6a was converted to the desired *E*-isomer using a palladium catalyzed isomerisation process [29]. Compound 6b was then converted exclusively to the enantiomerically pure (>99% ee) phthalide 7 via Sharpless asymmetric dihydroxylation using AD mix- β followed by *in-situ* cyclization with the cyano group [28]. We were also able to obtain an X-ray crystal structure¹ for 7 (Figure 2). Conversion of 7 to the target molecule 9 via a sequence of tosylation, azide displacement and reduction failed, and only the undesired compound 8 was isolated in 65% yield. It is worth mentioning that treatment of 7 with triflic anhydride in pyridine or diphenyl phospheryl azide (DPPA) led to the formation of 8 in comparable yield.

¹ A Crystallographic Information File (CIF) for the structure of compound 7 is available as supporting information. The crystallographic data are also available free of charge from the Cambridge Crystallographic Data Center (<http://www.ccdc.cam.ac.uk>) using the registry number CCDC 1433128.



Scheme 1: Preparation of compound 8. Reagents and conditions: **a.** Br₂, Fe powder, NaOAc, AcOH, 1.5 h (83%); **b.** NaH, CH₃I, DMF, rt, 15 h (76%); **c.** PBr₃, DCM, rt, 2 h (96%); **d.** PPh₃, toluene, rt, 3.5 h (97%); **e.** *n*-BuLi, THF, 0°C (30 min) - rt (14 h), then CuCN, DMF, reflux, 16 h (**6a**, 48% and **6b**, 32%); **f.** PdCl₂(PPh₃)₂, (EtO)₃SiH, THF, reflux, 15 h (85%); **g.** K₂Fe(CN)₆, K₂CO₃, (DHDQ)₂PHAL, K₂OSO₄·2 H₂O, THF, *t*-BuOH, H₂O (70%); **h.** TsCl, pyridine, DCM, rt, 3 h (65%).

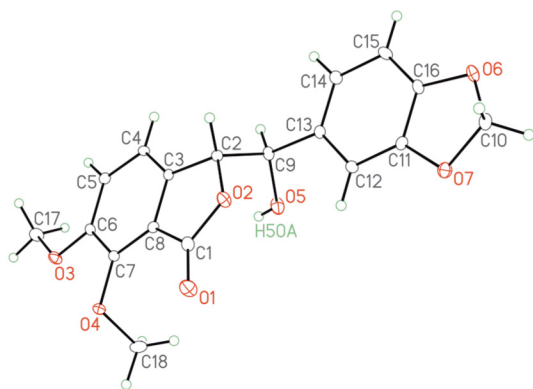


Figure 2: X-ray crystal structure for the alcohol 7.

The effect of the new compound (8) on MT polymerization

To determine the effect of noscapine and compound 8 upon the assembly of tubulin subunits into microtubules, changes in the turbidity of tubulin solution were measured in the absence or presence of the tested compounds. The control (tubulin in the prepared buffer with DMSO) represents the normal polymerization of microtubules in the absence of any added compounds at 37°C (Figure 3). Paclitaxel, a known microtubule stabilizer, is used to represent MT polymerization. Noscapine is known to stabilize MT leading to their polymerization [3], however to a lesser extent compared to paclitaxel (Figure 3). We

were expecting compound 8 to have a similar effect on MT polymerization as noscapine, however it was found to destabilize MT (Figure 3). These results suggest a different mechanism of action for compound 8 than noscapine.

Binding affinity of the new compound (8)

To test whether noscapine and compound 8 interact directly with tubulin, the fluorescence of α,β -tubulin heterodimers was examined in the presence and absence of noscapine, as well as compound 8. Interestingly, recombinant purified β I-tubulin was found to form homodimers, which gave the same characteristic bell-shaped tryptophan fluorescence with significant quenching in the presence of different concentrations of the tested compounds. The homodimer formation was confirmed by running native gel electrophoresis using a 10 μ L solution containing 30 μ g of the purified recombinant β I-tubulin (Figure 4).

The effect of both noscapine and compound 8 were tested on α I, β I-tubulin heterodimers, α I, β III-tubulin heterodimers, β I, β I-tubulin homodimers and porcine brain tubulin (unfractionated) to observe if there are any isotype-specific effects. Both compounds displayed notable quenching of tryptophan fluorescence in a concentration-dependent manner (Figure 5 and Table 1); however compound 8 showed a stronger quenching profile. These fluorescence quenching studies indicated that the ability of compound 8 to induce conformational changes upon binding varies depending on the tubulin isoform. The

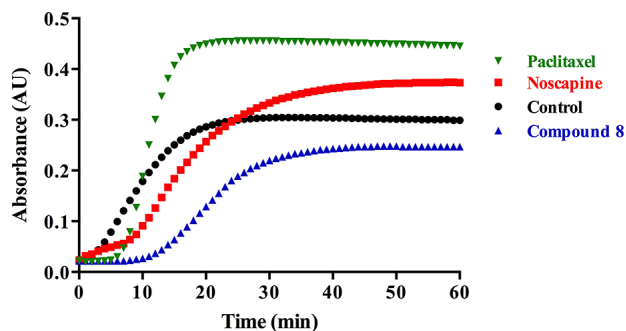


Figure 3: Microtubule assembly assay in the presence of noscapine, compound 8 or paclitaxel.

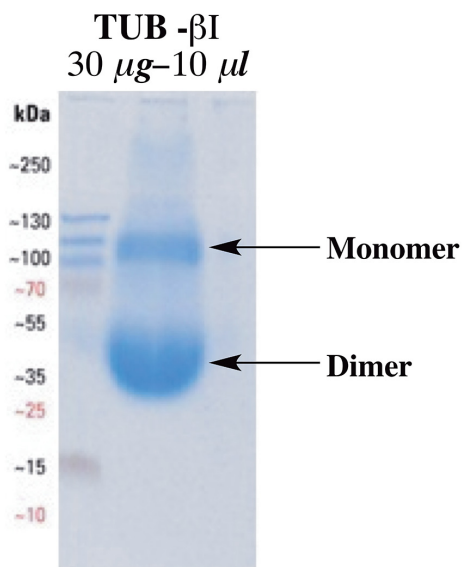


Figure 4: Native gel electrophoresis for the purified recombinant β I-tubulin at neutral pH using non-reducing loading buffer.

α I, β III-tubulin isoform was found to be particularly affected, and it should be noted that β III-tubulin is highly expressed in resistant tumor cells [30].

Antiproliferative effect of the new compound (8)

Arresting breast cancer cell growth and viability is still a challenge especially in view of drug resistance [31,32], which calls for the development of appropriate new modalities of treatment. The effect of noscapine and compound 8 (Figure 6) on the viability of the human breast cancer cell lines SKBR-3, and paclitaxel-resistant SKBR-3 was investigated using the colorimetric MTT assay. This was motivated by the earlier studies discussed above that indicated noscapine may be suitable for drug development towards cancer chemotherapy with relatively low toxicity compared to other anti-mitotic agents. Our data revealed that compound 8 was more cytotoxic than noscapine on

the SKBR-3 cell line with an IC_{50} of $\sim 40 \mu M$ compared to $\sim 100 \mu M$ for noscapine (Figure 6a). The same effect was also observed when using the paclitaxel-resistant SKBR-3, where compound 8 showed an IC_{50} of $\sim 64 \mu M$ compared to $\sim 100 \mu M$ for noscapine (Figure 6b).

Determination of the binding site of the new compound (8) on tubulin

The above experimental results indicate that compound 8 is a microtubule-destabilizing agent (Figure 3), and therefore affects microtubules differently than noscapine. Although compound 8 is structurally similar to noscapine, it also shares some similarity with the microtubule-destabilizing agents colchicine and combretastatin A4, both of which are thought to bind to the colchicine domain located at the intra-dimer interface of $\alpha\beta$ -tubulin [33,34]. Furthermore, compound 8 has several features that match the pharmacophore for the colchicine site that was developed by Nguyen *et al.* based on the binding of colchicine, combretastatin A4 and other agents [35]. Therefore, we performed docking simulations to investigate the binding mode and the binding strength of these compounds to the colchicine binding site, and establish similarities in binding poses that may provide support for compound 8 binding to this site.

Docking scores indicate that colchicine binds with the greatest affinity, followed by combretastatin A4, while compound 8 has the lowest affinity for tubulin (Figure 7). The top-ranked docking poses for colchicine resemble the crystal structure pose, providing confidence in our docking protocols. Small variations exist in the orientation of the acetamide relative to the crystal structure, which has been previously shown to have high mobility in the binding site [36]. The top poses of the other ligands are also similar, which indicates a common binding motif can be established.

A comparison of the energy-minimized top docking pose for each of the three compounds indicates some variability (Figure 7). Both combretastatin A4 and compound 8 bind deeper into β -tubulin than colchicine, which supports previous work that found flexible ligands bind more deeply [36]. For each compound, the methoxy-containing A ring is directed into β -tubulin near Cys241, and overlap of these rings is observed for the compounds studied, as previously found for colchicine and combretastatin A4 [35,37,38]. The colchicine A ring has been identified as an essential feature of the pharmacophore [39]. However, no direct hydrogen bonds form between the protein and these methoxy groups. It is possible stability is gained from an S-H \cdots O or S-H \cdots π interaction between Cys241 and the A ring of the ligands. Interactions occur between the ligands and residues Lys254 and Lys352; ligand lone pairs are directed towards the lysine side chain amino group in the binding poses for all three ligands (Figure 7). However, colchicine is

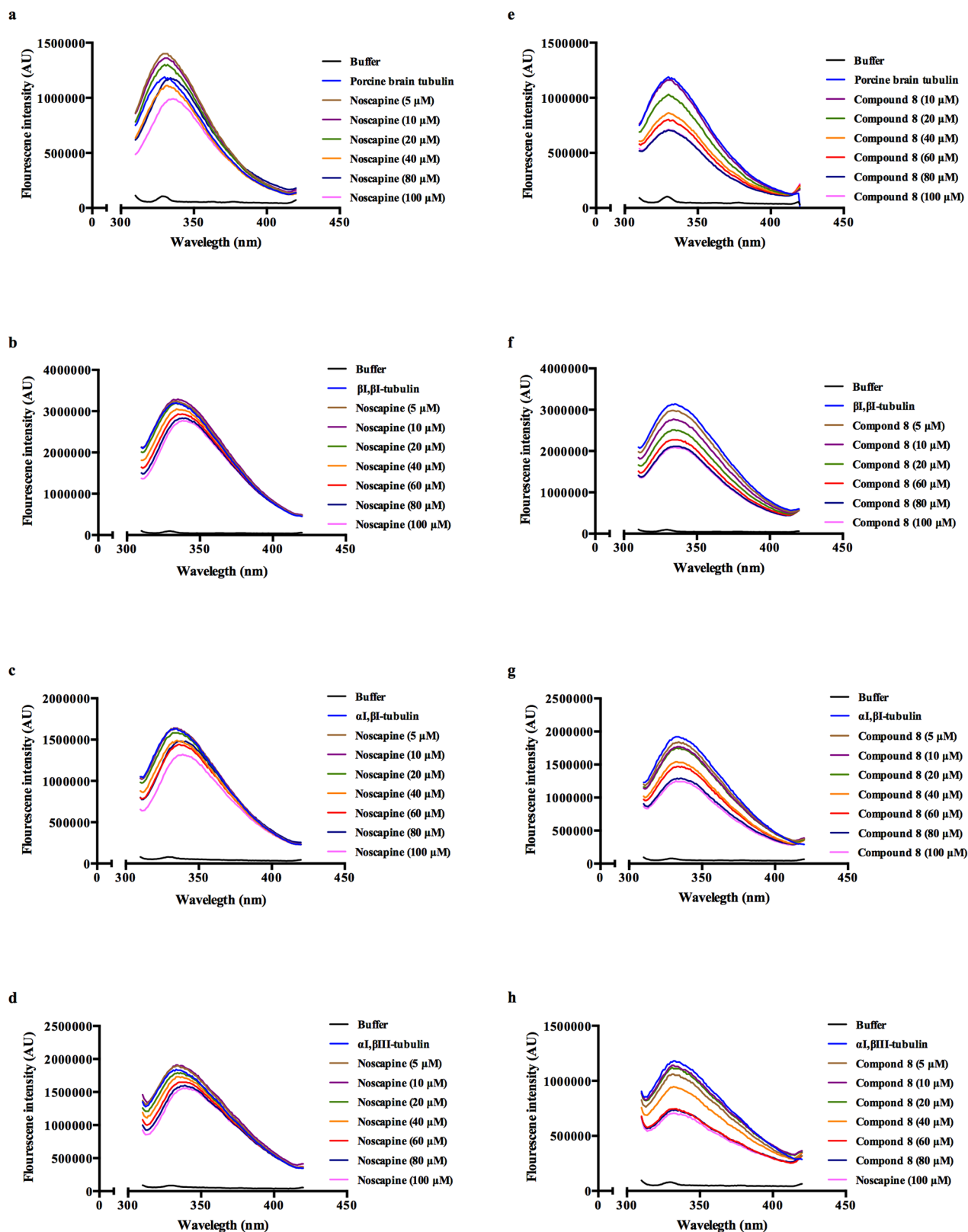


Figure 5: Fluorescence intensity quenching of noscapine a–d. and compound 8 e–h. using porcine brain tubulin (a,e), $\beta I, \beta I$ -tubulin (b,f), $\alpha I, \beta I$ -tubulin (c,g) and $\alpha I, \beta III$ -tubulin (d,h).

Table 1: Calculated binding affinity parameters; association (K_a , 10^3 M) and dissociation (K_d , μ M) constants for noscapine and compound 8 with porcine brain tubulin and purified recombinant tubulin dimers (β I, β I-tubulin, α I, β I-tubulin and α I, β III-tubulin) determined using a fluorescence quenching assay

| Compound Name | K_a (10^3 M) and K_d (μ M) | | | | | | | |
|---------------|--|--------|------------------------------|--------|-------------------------------|--------|---------------------------------|--------|
| | Porcine brain tubulin | | β I, β I-tubulin | | α I, β I-tubulin | | α I, β III-tubulin | |
| | K_a | K_d | K_a | K_d | K_a | K_d | K_a | K_d |
| Noscapine | 3.77 ± 0.02 | 265.25 | 2.35 ± 0.04 | 425.53 | 3.41 ± 0.04 | 293.25 | 3.46 ± 0.01 | 289.02 |
| Compound 8 | 5.75 ± 0.02 | 114.28 | $6.12 \pm$ | 163.39 | 5.78 ± 0.03 | 173.01 | 8.28 ± 0.10 | 121.06 |

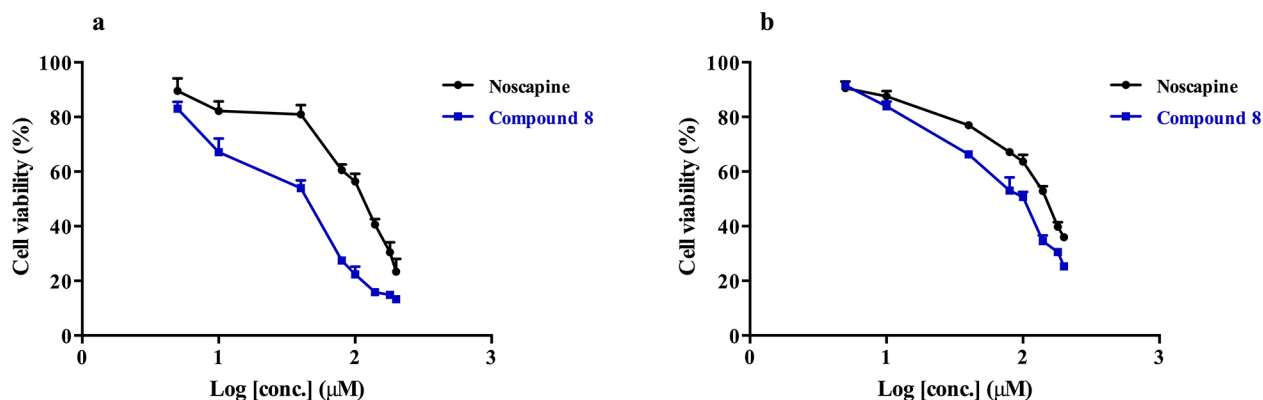


Figure 6: The effect of noscapine and compound 8 on the viability of breast cancer cell line **a.** SKBR-3; and **b.** paclitaxel resistant SKBR-3 using an MTT assay. Statistical analysis showed a statistically significant difference in the cytotoxicity of the compounds on both cell lines (p value < 0.05).

positioned closest to these lysine residues, compared to the other ligands. Arg258 is also in a position to interact with the ligands. These features indicate that compound 8 binds to the colchicine site in a fashion similar to that of other known colchicine-domain ligands.

DISCUSSION

This paper reports the results of synthesis, *in vitro* testing and *in silico* modeling of a novel noscapine analogue **8**. Noscapine has been repurposed from its original application as an anti-tussive agent to a cancer chemotherapy, particularly as a second line of treatment [40]. Unfortunately, while showing low toxicity, it also failed to demonstrate sufficient efficacy in clinical trials [41], although it shows some promise as a prophylactic agent [42]. In this paper, we focused on an analogue of noscapine that was synthesized in the hope of improving its cytotoxicity profile compared to the parent compound.

In MTT assays involving both SKBR-3 and the paclitaxel-resistant SKBR-3 breast cancer cell line, both noscapine and compound 8 show cytotoxic activity in the sub-mM range, with compound 8 being demonstrably more potent. Noscapine had IC₅₀ of ~ 100 for both cell lines, however compound 8 showed lower

IC₅₀ values of ~ 40 μ M and 64 μ M for the normal and the resistant SKBR-3 cell lines respectively. These cytotoxicity results were confirmed by the fluorescence quenching assays, which showed that compound 8 has lower K_d values, thus higher binding affinity, than its parent noscapine towards tubulin. The fluorescence quenching assays were done on porcine brain tubulin as well as purified recombinant tubulin dimers (β I, β I-tubulin, α I, β I-tubulin and α I, β III-tubulin). All tubulin isoforms showed similar results confirming the stronger binding of compound 8 towards tubulin. To determine the effect of compound 8 on microtubules, whether it stabilizes or destabilizes their polymerization, we did a MT polymerization assay using both compound 8 as well as noscapine. Noscapine is a known MT stabilizer that enhances the polymerization of MT. Interestingly, in contrast to noscapine, we found that compound 8 has strong microtubule-destabilizing properties. This surprising result suggest a different mechanism of action for compound 8, which might be due to a different binding site on the α , β -tubulin protein.

To have a deep insight on the binding site and mode of this compound to α , β -tubulin, we performed docking calculations for both compound 8 and noscapine towards both the colchicine as well as the noscapine binding sites.

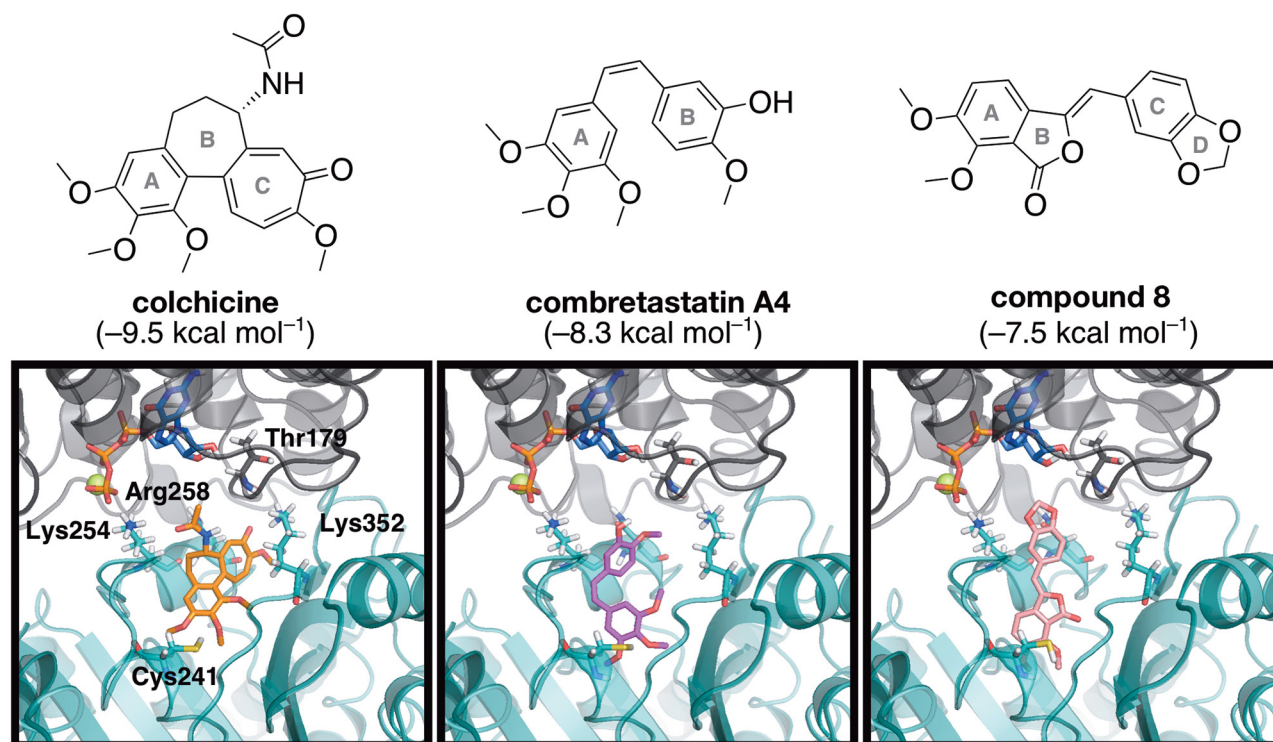


Figure 7: The energy-minimized docking poses of colchicine (orange), combretastatin A4 (magenta) and compound 8 (pink) in the colchicine binding domain located at the interdimer interface between α -tubulin (grey) and β -tubulin (teal). The nearby GTP and Mg²⁺ are shown in blue and yellow, respectively. Select residues are shown in stick mode, and labeled according to the numbering in the 1SA0 crystal structure. Docking scores (kcal mol^{−1}) are indicated in brackets.

These calculations have illustrated the binding mode of compound 8 to α,β -tubulin at the colchicine binding site, which we have shown is similar to that of other colchicine domain binders. This finding is consistent with structural features of compound 8 that have strong similarity with colchicine. It appears, therefore, that starting from the nescapine scaffold one can design compounds that gradually lose affinity for the nescapine-binding site and acquire propensity to bind to the colchicine binding site. Concomitant with this, there is a change in the mode of action of the compound, from stabilizing microtubules to destabilizing microtubules. It's worth mentioning that although compound 8 possesses low potency, it can be used in combination with other chemotherapeutic agents (paclitaxel) due to its low toxicity to get a synergistic effect and overcome cancer resistance. Similar effects were observed for paclitaxel when used in combination with the reduced 5-bromonescapine analogue [43,44]. Therefore further exploration of this new scaffold is required for the development of more potent tubulin binders.

MATERIALS AND METHODS

Materials

Nescapine and guanosine 5'-triphosphate (GTP) sodium salt hydrate were purchased from Sigma Aldrich,

Canada Co. The nescapine stock solution was prepared at 2 mM in dimethyl sulfoxide (DMSO) and kept at -20°C. Porcine brain tubulin (Cat.# T240-DX) was purchased from Cytoskeleton Inc. The genes for human α I-, β I- and β III-tubulin were purchased from DNA2.0 (Menlo Park, CA, USA). All reagents were purchased from Sigma-Aldrich Canada Ltd. (Oakville, Ontario, Canada) and Fisher Scientific Company (Ottawa, Ontario, Canada). Nickel-NTA resin was purchased from Qiagen Inc. (Toronto, Ontario, Canada).

Methods

General procedure for chemical synthesis

Reactions were carried out in flame-dried glassware under a positive argon atmosphere unless otherwise stated. Transfer of anhydrous solvents and reagents was accomplished with oven-dried syringes or cannulae. Solvents were distilled before use: dichloromethane (CH₂Cl₂) and dimethylformamide (DMF) from calcium hydride, tetrahydrofuran (THF), and toluene from sodium/benzophenone ketyl and pyridine from KOH. Thin layer chromatography was performed on glass plates precoated with 0.25 mm silica. Flash chromatography columns were packed with 230–400 mesh silica gel. Optical rotations were measured using a Perkin Elmer 241 Polarimeter at 22 ± 2 °C. Proton nuclear magnetic resonance spectra

(¹H NMR) were recorded at 500 MHz and coupling constants (J) are reported in hertz (Hz). Standard notation was used to describe the multiplicity of signals observed in ¹H NMR spectra: broad (br), multiplet (m), singlet (s), doublet (d), triplet (t), etc. Carbon nuclear magnetic resonance spectra (¹³C NMR) were recorded at 125 MHz and are reported (ppm) relative to the centerline of the triplet from chloroform-d (77.0 ppm), or the centerline of the heptuplet from methanol-d₄ (49.0 ppm). Infrared (IR) were measured using a Thermo Nicolet 8700 main bench with an attached Continuum FTIR microscope. Mass spectra were determined on a high-resolution electrospray positive ion mode spectrometer. Melting points were measured using the Thomas Hoover Capillary Melting Point Apparatus.

Procedure for the synthesis of 2-bromo-3,4-dimethoxybenzaldehyde (**3**)

NaH (1.32 g, 32.9 mmol) was added to a stirred solution of 2-bromo-3-hydroxy-4-methoxybenzaldehyde **2** [25] (6.30 g, 27.4 mmol) in anhydrous DMF (80 mL) at 0 °C for 15 min. CH₃I (2.05 mL, 32.9 mmol) was then added as a single portion to the reaction mixture and left to stir at room temperature for 15 h. The solvent was evaporated under reduced pressure to give the crude product, which was then dissolved in CH₂Cl₂, washed with water, brine, and dried over Na₂SO₄. The organic layer was filtered, concentrated under reduced pressure, and then purified by column chromatography on silica gel using 20% EtOAc/hexane as the eluent to afford **3** (5.07 g, 20.8 mmol, 76% yield) as a white solid that matched previously reported characterization data [26]: ¹H NMR (500 MHz, CDCl₃) δ 10.26 (d, *J* = 0.5 Hz, 1H), 7.75 (d, *J* = 11.0 Hz, 1H), 6.96 (d, *J* = 11.0, 0.5 Hz, 1H), 3.96 (s, 3H), 3.89 (s, 3H).

Procedure for the synthesis of (*E/Z*)-6-(2-(benzo[*d*][1,3]dioxol-5-yl)vinyl)-2,3-dimethoxybenzonitrile (**6a/6b**)

n-Butyllithium in hexane (2.1 M, 7.01 mL, 14.7 mmol) was added dropwise to a stirred solution of **5** [27] (6.99 g, 14.7 mmol) in anhydrous THF (30 mL) at 0 °C. The solution was stirred for 30 min at 0 °C, then 2-bromo-3,4-dimethoxybenzaldehyde **3** (3.41 g, 14.0 mmol) in THF (15 mL) was added dropwise via syringe at the same temperature. The reaction mixture was allowed to stir for 14 h at room temperature (monitored by TLC). The reaction mixture was then cooled to 0 °C, and saturated solution of NH₄Cl (25 mL) was added. The aqueous layer was separated and extracted with CH₂Cl₂ (3 × 25 mL). The organic layers were combined, washed with water, brine, dried over anhydrous Na₂SO₄, filtered, and concentrated under reduced pressure to give the crude product as a mixture of *E/Z*. The crude product was then dissolved in DMF (40 mL) at room temperature. CuCN (1.88 g, 21.0 mmol) was then added to the reaction mixture, which was then refluxed for 16 h. The reaction mixture was then cooled down to room temperature before adding H₂O (20

mL). Next, the aqueous layer was separated and extracted with CH₂Cl₂ (3 × 25 mL). The organic layers were combined, washed with water, brine, dried over anhydrous Na₂SO₄, and concentrated under reduced pressure then purified by column chromatography on silica gel using 30% EtOAc/hexane as the eluent to afford both *E*- and *Z*- isomers in 48% (2.07 g, 6.72 mmol) and 32% (1.38 g, 4.48 mmol) isolated yields respectively.

(*Z*)-6-(2-(benzo[*d*][1,3]dioxol-5-yl)vinyl)-2,3-dimethoxybenzonitrile (**6a**)

Pale yellow oil; *R_f* = 0.30 (70:30 Hexane: Ethyl acetate); IR (cast film) ν_{\max} = 3011, 2944, 2900, 2840, 2227, 1595, 1565, 1492, 1446, 1417, 1353, 1266, 1239, 1214, 1194, 1180, 1091, 1073, 1039 cm⁻¹; ¹H NMR (500 MHz, CDCl₃) δ 7.02 (dd, *J* = 8.5, 0.5 Hz, 1H), 6.92 (d, *J* = 8.5 Hz, 1H), 6.67-6.66 (m, 2H), 6.60 (d, *J* = 12.0 Hz, 1H), 6.60-6.59 (m, 1H), 6.5 (d, *J* = 12.0 Hz, 1H), 5.87 (s, 2H), 3.98 (s, 3H), 3.83 (s, 3H); ¹³C NMR (125 MHz, CDCl₃) δ 151.7, 151.2, 147.5, 147.1, 133.4, 132.7, 130.2, 125.0, 124.3, 123.3, 116.6, 115.1, 108.6, 108.3, 107.4, 101.1, 61.6, 56.1; HRMS (ESI) calcd for C₁₈H₁₅NNaO₄ [M + Na]⁺ 332.0893; found 332.0892.

(*E*)-6-(2-(benzo[*d*][1,3]dioxol-5-yl)vinyl)-2,3-dimethoxybenzonitrile (**6b**)

White solid; mp 129-131 °C; *R_f* = 0.21 (70:30 Hexane: Ethyl acetate); IR (cast film) ν_{\max} = 3005, 2943, 2903, 2841, 2225, 1632, 1604, 1593, 1565, 1494, 1449, 1416, 1361, 1295, 1278, 1253, 1233, 1198, 1124, 1098, 1074 cm⁻¹; ¹H NMR (500 MHz, CDCl₃) δ 7.41 (d, *J* = 9.0 Hz, 1H), 7.14 (d, *J* = 16.0 Hz, 1H), 7.11 (d, *J* = 9.0 Hz, 1H), 7.08 (d, *J* = 1.5 Hz, 1H), 7.04 (d, *J* = 16.0 Hz, 1H), 6.96 (dd, *J* = 8.0, 1.5 Hz, 1H), 6.80 (d, *J* = 8.0 Hz, 1H), 5.99 (s, 2H), 4.03 (s, 3H), 3.91 (s, 3H); ¹³C NMR (125 MHz, CDCl₃) δ 151.7, 151.3, 148.3, 148.0, 133.6, 131.2, 131.0, 122.1, 122.0, 120.5, 117.2, 115.2, 108.5, 106.5, 105.8, 101.3, 61.7, 56.3; HRMS (ESI) calcd for C₁₈H₁₅NNaO₄ [M + Na]⁺ 332.0893; found 332.0895.

Procedure for the synthesis of (*R*)-3-((*R*)-benzo[*d*][1,3]dioxol-5-yl(hydroxy)methyl)-6,7-dimethoxyisobenzofuran-1(3H)-one (**7**)

K₃Fe(CN)₆ (3.68 g, 11.2 mmol) and K₂CO₃ (1.55 g, 11.2 mmol) were added to a solution of *t*-BuOH (10 mL), THF (10 mL) and H₂O (20 mL) and stirred for 10 min at room temperature. (DHQD)₂PHAL [28] (26.5 mg, 1.0 mol%) and K₂OsO₄·2H₂O (12.5 mg, 1.0 mol%) were then added and stirring of the mixture was continued for 30 min at room temperature. To the stirring reaction mixture was then added compound **6b** (1.1 g, 3.4 mmol). After stirring for 18 h at room temperature, sodium bisulphite (3.0 g, 28.8 mmol) and H₂O (10 mL) were added and the reaction mixture was stirred for further 2 h. The aqueous layer was then separated and extracted with CH₂Cl₂ (3 × 25 mL). The organic layers were combined, washed with water, brine, dried over anhydrous Na₂SO₄, filtered and concentrated under reduced pressure then purified by

column chromatography on silica gel using 40% EtOAc/hexane as the eluent to afford **7** (0.83 g, 2.4 mmol, 70% yield) as white solid; mp 153–155 °C; >99% ee by chiral HPLC analysis (Chiracel AD-H, n-hexane–iPrOH, 80:20, 1 mL min⁻¹) retention time 42.47 (>99%); $R_f = 0.67$ (20:80 Hexane: Ethyl acetate); $[\alpha]_D^{20} + 14.66$ (c 0.15, DCM); IR (cast film) $\nu_{\max} = 3479, 3068, 2934, 2852, 1759, 1598, 1501, 1444, 1425, 1350, 1272, 1252, 1194, 1165, 1117, 1099, 1037$ cm⁻¹; ¹H NMR (500 MHz, CD₃OD) δ 7.30 (d, $J = 8.5$ Hz, 1H), 6.87 (dd, $J = 8.5, 1.0$ Hz, 1H), 6.79 (d, $J = 1.5$ Hz, 1H), 6.75 (dd, $J = 8.0, 1.5$ Hz, 1H), 6.72 (d, $J = 8.0$ Hz, 1H), 5.91 (d, $J = 1.0$ Hz, 1H), 5.90 (d, $J = 1.0$ Hz, 1H), 5.53 (dd, $J = 5.5, 1.0$ Hz, 1H), 4.85 (d, $J = 5.5$ Hz, 1H), 3.90 (s, 3H), 3.86 (s, 3H), (OH proton could not be observed in CD₃OD); ¹³C NMR (125 MHz, CD₃OD) δ 170.1, 154.1, 149.0, 148.9, 148.9, 141.2, 134.5, 122.2, 120.8, 120.1, 119.8, 108.8, 108.6, 102.4, 84.2, 75.7, 62.4, 57.3; HRMS (ESI) calcd for C₁₈H₁₆NaO₇[M + Na]⁺ 367.0788; found 367.0785.

Procedure for the synthesis of (Z)-3-(benzo[d][1,3]dioxol-5-ylmethylene)-6,7-dimethoxyisobenzofuran-1(3H)-one (**8**)

p-Toluenesulfonyl chloride (0.13 g, 0.67 mmol) was added portionwise to a solution of **7** (0.21 g, 0.61 mmol) and pyridine (74.4 μ L, 0.92 mmol) in DCM (10 mL) at room temperature. After stirring for 2 h at room temperature, water (5 mL) was added and the solution was extracted with CH₂Cl₂ (3 x 10 mL). The organic layers were combined, washed with water, brine, dried over anhydrous Na₂SO₄, filtered and concentrated under reduced pressure then purified by column chromatography on silica gel using 50% EtOAc/hexane as the eluent to afford **8** (0.13 g, 0.40 mmol, 65% yield) as yellow solid; mp 159–161 °C; $R_f = 0.37$ (60:40 Hexane: Ethyl acetate) IR (cast film) $\nu_{\max} = 3064, 3008, 2954, 2927, 2856, 1771, 1758, 1732, 1664, 1616, 1596, 1502, 1447, 1365, 1350, 1279, 1258, 1198, 1167, 1139, 1127, 1109, 1076, 1040, 1026$ cm⁻¹; ¹H NMR (500 MHz, CDCl₃) δ 7.51 (d, $J = 2.0$ Hz, 1H), 7.38 (d, $J = 8.5$ Hz, 1H), 7.28 (d, $J = 8.5$ Hz, 1H), 7.19 (dd, $J = 8.5, 2.0$ Hz, 1H), 6.85 (d, $J = 8.5$ Hz, 1H), 6.21 (s, 1H), 6.02 (s, 2H), 4.18 (s, 3H), 3.97 (s, 3H); ¹³C NMR (125 MHz, CDCl₃) δ 164.6, 152.9, 148.2, 148.1, 147.5, 142.8, 134.2, 127.8, 124.5, 120.0, 115.4, 114.4, 109.6, 108.5, 104.9, 101.3, 62.4, 57.0; HRMS (ESI) calcd for C₁₈H₁₄NaO₆ [M + Na]⁺ 349.0683; found 349.0681.

Microtubule assembly assay

The turbidity was recorded on 96-half area well plates by microplate reader at 340 nm as an indicator for microtubules formation. The wells containing 80 mM piperazine-N,N'-bis[2-ethanesulfonic acid] sequisodium salt (PIPES buffer, pH 6.9); 2.0 mM MgCl₂; 0.5 mM ethylene glycol-bis(β -amino-ethyl ether) N,N,N',N'-tetraacetic acid (EGTA), 10 μ M of noscapine or compound **8** in DMSO were kept at room temperature. Tubulin at a

concentration of 3mg/mL in tubulin buffer (80 mM PIPES pH 6.9, 2 mM MgCl₂, 0.5 mM EGTA, 1 mM GTP, 10.2% glycerol) was kept at 4 °C before being added to the wells and shifting to 37°C. The absorbance was measured using the kinetic absorbance mode. DMSO solutions of paclitaxel and colchicine (10 μ M) were used as controls.

Preparation of human α I-, β I- and β III-tubulin

The protein sequence of human α I-tubulin is given by UniProtKB accession number Q71U36 (gene name TUBA1A), the protein sequence of human β I-tubulin is given by UniProtKB accession number P07437 (gene name TUBB) and that of human β III-tubulin is given by UniProtKB accession number Q13509 (gene name TUBB3). The cloning work for α I- and β I-tubulin was performed and reported previously [45]. For the β III human tubulin protein, the sequence was converted into DNA sequences with codons optimized for production in *Escherichia coli*, and for purification purposes, a His-tag was added at the N-terminus. The β III-tubulin gene was inserted into a pET15b vector between the XhoI and NdeI restriction sites. The correct sequence, insertion, and orientation of the tubulin constructs were verified by DNA sequencing. Recombinant proteins were expressed in *E. coli* BL21 (DE3) host cells in LB medium supplemented with 100 μ g/mL ampicillin. The cultures were grown at 37 °C until an OD600 = 0.8 was reached, and the cells were induced with 1.0 mM isopropyl b-D-1-thiogalactopyranoside (IPTG) for 18 h at 25 °C. After induction, the cells were harvested by centrifugation (6000 \times g for 20 min at 4 °C in SLC-6000 evolution sorvall rotor). The three variants of the tubulin protein were isolated from the inclusion bodies.

The α I-, β I- and β III-tubulin constructs were purified in the same manner *via* fast refolding by dilution with metal affinity chromatography (IMAC) using a Ni-NTA column. The cell pellets from 1 L of the LB medium with expressed tubulin protein were resuspended in 25 mL of buffer A (buffer A: 50 mM Tris, 50 mM MgSO₄, 50 mM NaCl, pH 8.8) and lysed by sonication (using Fisher Scientific Ultrasonic Dismembrator Model 500 with microtip probe for 4 times (30 seconds each) pulses at 45% power) on ice followed by centrifugation at 12000 \times g for 20 min (4 °C) in JA 25–50 fixed angle rotor, Beckman Coulter centrifuge. The supernatant was removed, and the inclusion bodies were cleaned by a series of washing steps with buffer A containing 0.1% Triton X-100, 25% glycerol, 500 mM NaCl, and 2 M urea as a separate additive for every next wash. Inclusion bodies were centrifuged at 12,000 \times g for 20 min (4 °C) in JA 25–50 rotor after every wash, and the supernatant was removed. The clean protein pellet was solubilized in buffer B (buffer B: 50 mM Tris 50 mM NaCl, 1 mM CaCl₂, 8 M urea, 10 mM beta-mercaptoethanol, pH 8.8) and left for slowly rotated incubation at room temperature overnight. The next day, the sample was centrifuged at 33,000 \times g for 1 h (25 °C) in a JA 25–50 rotor. The tubulin proteins were refolded *via* rapid dilution (1:10

volume/volume) into buffer C (buffer C: 50 mM Tris, 50 mM NaCl, 10 mM MgSO₄, 1 mM CaCl₂, pH 7.4) and loaded onto a Ni-NTA column (25 mL bed volume) pre-equilibrated with buffer C. The loaded sample was incubated on a column for 1 h (4 °C) with rotation. The column was then washed with buffer D (buffer D: 50 mM Tris, 50 mM NaCl, 10 mM MgSO₄, 1 mM CaCl₂, 10 mM imidazole, pH 7.3), and tubulins were eluted with a linear gradient of 500 mM imidazole in buffer D. Fractions containing the protein were identified by spot testing and SDS-PAGE gel, then mixed followed by overnight dialysis (4 °C with two buffer changes) against 10 volumes of buffer E (buffer E: 25 mM Tris, 25 mM NaCl, 10 mM MgSO₄, 1 mM MgCl₂, 1 mM CaCl₂, pH 7.3). The protein concentration (μM) was determined using the corresponding extinction coefficient at 280 nm (αI-tubulin: 51060 M⁻¹cm⁻¹, βI-tubulin: 46340 M⁻¹ cm⁻¹ and βIII-tubulin: 47832 M⁻¹ cm⁻¹) calculated by the ProtParam software based on recombinant αI-, βI- and βIII-tubulin amino acid sequences. The three proteins were then concentrated using an Amicon Ultra-15 centrifugal device.

Binding experiments and tryptophan fluorescence quenching assays

In a 96-well microplate, equimolar mixtures of recombinant human tubulin monomers, as well as buffer (10 mM sodium phosphate, 10 mM MgCl₂, 1 mM GTP, 0.5% DMSO, 250 mM sucrose, pH 7.0) were combined to reach a final tubulin dimer concentration of 2 μM for βI,βI-tubulin, αI,βI-tubulin and αI,βIII-tubulin. GTP was added to the samples to a final concentration of 1 mM. The microplate was incubated on ice for 10 min to allow for the formation of the tubulin dimer. The calculated amounts of stock solution of the compounds in DMSO were added to the protein samples to obtain final ligand concentrations of 5, 10, 20, 40, 60, 80 and 100 μM. The control was ligand-free, and the total sample volume was 100 μL. A glass bead was inserted into each well, and the microplate was covered with protective film, sealed with a lid, and incubated for 30 min at 25 °C. After that time, the microplate was transferred to a rotating plate form and vigorously rotated for 1 h at room temperature. From each well, 80 μL of samples and control were transferred to a 1 cm fluorescence cell. Fluorescence spectra were collected on a PTI MODEL-MP1 spectrofluorometer using a 10 mm path length cell at 295 nm (excitation wavelength) and a scan range of 310–400 nm. Data analysis was performed using ORIGIN 6.1 software (Origin-Lab, Northampton, MA, USA).

Determination of binding affinity parameters

The apparent binding constant of noscapine and compound 8 to different tubulin isoforms was calculated using data from the fluorescence experiments via the Stern–Volmer equation [46]:

$$(F_0 - F) / F = K_a [L]_a \quad (1)$$

where F_0 and F are the fluorescence intensities in the absence and in the presence of quencher respectively, K_a is the formation constant of the donor–acceptor (quencher–fluorogen) complex, and $[L]_a$ is the concentration of the tested compound added. Excitation and emission slits were set at 4 nm. All spectra were collected with samples having final optical densities (1 cm) < 0.3 at maximum absorbance of added ligand and were corrected for the inner filter effect according to equation 2 [47]:

$$F_{\text{corr}} = F_{\text{obs}} \times [10]^{(A_{\text{ex}} + A_{\text{em}}) / 2} \quad (2)$$

where F_{corr} is the corrected fluorescence, F_{obs} is the measured fluorescence, A_{ex} is the absorption value at the excitation wavelength (295 nm), and A_{em} is the absorption value at the emission wavelength (336 nm). From the slope of the linear plot of $((F_0 - F)/F)$ versus $[L]_a$, binding constants were estimated. The results are expressed as mean values SD (n=4).

Cell culture

The human breast cancer cell lines SKBR-3 and paclitaxel-resistant SKBR-3 were kindly provided by Marc St. George (University of Alberta, Canada) [48]. Both cell lines were grown in RPMI 1640 medium (GIBCO) with 10% fetal calf serum and 1 mM L-glutamine 1% penicillin/streptomycin mixture under a humidified atmosphere containing 5% CO₂. Addition of 16.65 nM paclitaxel to the paclitaxel-resistant cell line is mandatory to keep the acquired resistance at the same efficiency level.

MTT assay

The human breast cancer cell lines SKBR-3 and paclitaxel-resistant SKBR-3 (1 × 10⁴ cells per well) were seeded into 96-well plates. After incubation for 24 h (when cells reached 70–80% confluency), the medium was aspirated and the cells were treated with several concentrations of noscapine, as well as compound 8. After 21 h incubation, 50 μL of MTT (1 mg/mL) solution was added and the plates were incubated for an additional 3 h. After centrifugation, supernatant was removed from each well and 150 μL of dimethyl sulfoxide (DMSO) was added to dissolve the insoluble formazan crystals. The absorbance was measured at 570 nm and 690 nm subtracted as a background, using microplate reader. The data was plotted using GraphPad Prism 5.0 software. IC₅₀ and statistical analysis (t-test) were calculated using the same software.

Computational details of the docking calculations

Colchicine, combretastatin A4 and compound 8 were docked to the colchicine binding site. Receptor coordinates were obtained from the 1SA0 crystal structure [30] in the Protein Data Bank (PDB). To prepare the αβ-tubulin

heterodimer for docking, hydrogen atoms were added by the tleap module of AmberTools [49] and the Protonate 3D tool in the Molecular Operating Environment (MOE) software program [50] Nucleotide cofactors and magnesium ions were retained. Subsequently, this complex was energy minimized using the Amber12:EHT force field in MOE.

Using the MOE program, compounds were docked to the receptor at the colchicine site identified in the 1SA0 structure. An induced fit protocol was used for docking calculations. The receptor was defined as the protein, nucleotide cofactors and Mg²⁺ ions. Receptor atoms belonging to residues within 4.5 Å from the crystalized colchicine coordinates were allowed to move during docking. Docking poses were first scored with the London dG method and the top 30 unique hits were rescored with the GBVI/WSA dG methods, where the top 10 unique hits were retained. Duplicate poses were discarded. Following the docking calculations, the ligand-receptor complex for the top pose of each compound was energy minimized using the Amber12:EHT force field in MOE to maximize ligand-receptor interactions.

ACKNOWLEDGMENTS

The authors would like to thank Gareth Lambkin for his help with the cell culture.

CONFLICTS OF INTEREST

The authors of this manuscript declare no conflict of interest.

GRANT SUPPORT

This work was supported by grants from NSERC (Canada), Alberta Cancer Foundation, the Canadian Breast Cancer Foundation, the Allard Foundation and the University of Alberta.

REFERENCES

1. Robiquet P. Observations sur le mémoire de M. Sertuerner relatif à l'analyse de l'opium. *Ann Chim Phys.* 1817; 12:275–288.
2. Winter CA, Flataker L. Toxicity studies on noscapine. *Toxicol Appl Pharmacol.* 1961; 3:96–106.
3. Ye K, Ke Y, Keshava N, Shanks J, Kapp JA, Tekmal RR, Petros J, Joshi HC. Opium alkaloid noscapine is an antitumor agent that arrests metaphase and induces apoptosis in dividing cells. *Proc Natl Acad Sci.* 1998; 95:1601–1606.
4. Ke Y, Ye K, Grossniklaus HE, Archer DR, Joshi HC, Kapp JA. Noscapine inhibits tumor growth with little toxicity to normal tissues or inhibition of immune responses. *Cancer Immunol Immunother.* 2000; 49:217–225.
5. Zhou J, Panda D, Landen JW, Wilson L, Joshi HC. Minor alteration of microtubule dynamics causes loss of tension across kinetochore pairs and activates the spindle checkpoint. *J Biol Chem.* 2002; 277:17200–17208.
6. Aneja R, Dhiman N, Idnani J, Awasthi A, Arora SK, Chandra R, Joshi HC. Preclinical pharmacokinetics and bioavailability of noscapine, a tubulin-binding anticancer agent. *Cancer Chemother Pharmacol.* 2007; 60:831–839.
7. Heidari N, Goliaei B, Moghaddam PR, Rahbar-Roshandel N, Mahmoudian M. Apoptotic pathway induced by noscapine in human myelogenous leukemic cells. *Anticancer Drugs.* 2007; 18:1139–1147.
8. Liu M, Luo X-J, Liao F, Lei X-F, Dong W-G. Noscapine induces mitochondria-mediated apoptosis in gastric cancer cells in vitro and in vivo. *Cancer Chemother Pharmacol.* 2011; 67:605–612.
9. Yang Z-R, Liu M, Peng X-L, Lei X-F, Zhang J-X, Dong W-G. Noscapine induces mitochondria-mediated apoptosis in human colon cancer cells in vivo and in vitro. *Biochem Biophys Res Commun.* 2012; 421:627–633.
10. Newcomb EW, Lukyanov Y, Smirnova I, Schnee T, Zagzag D. Noscapine induces apoptosis in human glioma cells by an apoptosis-inducing factor-dependent pathway. *Anticancer Drugs.* 2008; 19:553–563.
11. Verma AK, Bansal S, Singh J, Tiwari RK, Kasi Sankar V, Tandon V, Chandra R. Synthesis and in vitro cytotoxicity of haloderivatives of noscapine. *Bioorg Med Chem.* 2006; 14:6733–6736.
12. Naik PK, Chatterji BP, Vangapandu SN, Aneja R, Chandra R, Kantevari S, Joshi HC. Rational design, synthesis and biological evaluations of amino-noscapine: a high affinity tubulin-binding noscapinoid. *J Comput Aided Mol Des.* 2011; 25:443–454.
13. Aneja R, Vangapandu SN, Lopus M, Chandra R, Panda D, Joshi HC. Development of a novel nitro-derivative of noscapine for the potential treatment of drug-resistant ovarian cancer and T-cell lymphoma. *Mol Pharmacol.* 2006; 69:1801–1809.
14. Santoshi S, Naik PK, Joshi HC. Rational design of novel anti-microtubule agent (9-azido-noscapine) from quantitative structure activity relationship (QSAR) evaluation of noscapinoids. *J Biomol Screen.* 2011; 16:1047–1058.
15. Aneja R, Vangapandu SN, Joshi HC. Synthesis and biological evaluation of a cyclic ether fluorinated noscapine analog. *Bioorg Med Chem.* 2006; 14:8352–8358.
16. Mishra RC, Karna P, Gundala SR, Pannu V, Stanton RA, Gupta KK, Robinson MH, Lopus M, Wilson L, Henary M, Aneja R. Second generation benzofuranone ring substituted noscapine analogs: synthesis and biological evaluation. *Biochem Pharmacol.* 2011; 82:110–121.
17. Manchukonda NK, Naik PK, Santoshi S, Lopus M, Joseph S, Sridhar B, Kantevari S. Rational design, synthesis, and biological evaluation of third generation α -noscapine analogues as potent tubulin binding anti-cancer agents. *PLoS One.* 2013; 8:e77970.

18. Checchi PM, Nettles JH, Zhou J, Snyder JP, Joshi HC. Microtubule-interacting drugs for cancer treatment. *Trends Pharmacol Sci.* 2003; 24:361–365.
19. Rohena CC, Mooberry SL. Recent progress with microtubule stabilizers: new compounds, binding modes and cellular activities. *Nat Prod Rep.* 2014; 31:335–355.
20. Field JJ, Diaz JF, Miller JH. The binding sites of microtubule-stabilizing agents. *Chem Biol.* 2013; 20:301–315.
21. Lu Y, Chen J, Xiao M, Li W, Miller DD. An overview of tubulin inhibitors that interact with the colchicine binding site. *Pharm Res.* 2012; 29:2943–2971.
22. Naik PK, Santoshi S, Rai A, Joshi HC. Molecular modelling and competition binding study of Br-noscaptopine and colchicine provide insight into noscapinoid-tubulin binding site. *J Mol Graph Model.* 2011; 29:947–955.
23. Zhou J, Gupta K, Aggarwal S, Aneja R, Chandra R, Panda D, Joshi HC. Brominated derivatives of noscaptopine are potent microtubule-interfering agents that perturb mitosis and inhibit cell proliferation. *Mol Pharmacol.* 2003; 63:799–807.
24. Alisarai L, Tuszynski JA. Determination of noscaptopine's localization and interaction with the tubulin- α/β heterodimer. *Chem Biol Drug Des.* 2011; 78:535–546.
25. Hazlet SE, Brotherton RJ. Some Substitution Reactions of Isovanillin and Related Compounds. *J Org Chem.* 1962; 27:3253–3256.
26. Sinhababu AK, Borchardt RT. General method for the synthesis of phthalaldehydic acids and phthalides from o-bromobenzaldehydes via ortho-lithiated aminoalkoxides. *J Org Chem.* 1983; 48:2356–2360.
27. Aslam SN, Stevenson PC, Phythian SJ, Veitch NC, Hall DR. Synthesis of cicerfuran, an antifungal benzofuran, and some related analogues. *Tetrahedron.* 2006; 62:4214–4226.
28. Reddy RS, Kiran INC, Sudalai A. CN-assisted oxidative cyclization of cyano cinnamates and styrene derivatives: a facile entry to 3-substituted chiral phthalides. *Org Biomol Chem.* 2012; 10:3655–3661.
29. Bai X-F, Xu L-W, Zheng L-S, Jiang J-X, Lai G-Q, Shang J-Y. Aromatic-amide-derived olefins as a springboard: isomerization-initiated palladium-catalyzed hydrogenation of olefins and reductive decarbonylation of acyl chlorides with hydrosilane. *Chem. Eur. J.* 2012; 18:8174–8179.
30. Torin Huzil J, Ludueña RF, Tuszynski J. Comparative modelling of human β tubulin isoforms and implications for drug binding. *Nanotechnology.* 2006; 17:S90–100.
31. Browder T, Butterfield CE, Kråling BM, Shi B, Marshall B, O'Reilly MS, Folkman J. Antiangiogenic scheduling of chemotherapy improves efficacy against experimental drug-resistant cancer. *Cancer Res.* 2000; 60:1878–1886.
32. Chu F, Chou PM, Zheng X, Mirkin BL, Rebbaa A. Control of multidrug resistance gene *mdr1* and cancer resistance to chemotherapy by the longevity gene *sirt1*. *Cancer Res.* 2005; 65:10183–10187.
33. Prota AE, Danel F, Bachmann F, Bargsten K, Buey RM, Pohlmann J, Reinelt S, Lane H, Steinmetz MO. The Novel Microtubule-Destabilizing Drug BAL27862 Binds to the Colchicine Site of Tubulin with Distinct Effects on Microtubule Organization. *J Mol Biol.* 2014; 426:1848–1860.
34. Ravelli RBG, Gigant B, Curmi PA, Jourdain I, Lachkar S, Sobel A, Knossow M. Insight into tubulin regulation from a complex with colchicine and a stathmin-like domain. *Nature.* 2004; 428:198–202.
35. Nguyen TL, McGrath C, Hermone AR, Burnett JC, Zaharevitz DW, Day BW, Wipf P, Hamel E, Gussio R. A common pharmacophore for a diverse set of colchicine site inhibitors using a structure-based approach. *J Med Chem.* 2005; 48:6107–6116.
36. Chakraborti S, Chakravarty D, Gupta S, Chatterji BP, Dhar G, Poddar A, Panda D, Chakrabarti P, Ghosh Dastidar S, Bhattacharyya B. Discrimination of ligands with different flexibilities resulting from the plasticity of the binding site in tubulin. *Biochemistry.* 2012; 51:7138–7148.
37. Akselsen OW, Odlo K, Cheng J-J, Maccari G, Botta M, Hansen TV. Synthesis, biological evaluation and molecular modeling of 1,2,3-triazole analogs of combretastatin A-1. *Bioorg Med Chem.* 2012; 20:234–242.
38. Ducki S, Mackenzie G, Greedy B, Armitage S, Chabert JFD, Bennett E, Nettles J, Snyder JP, Lawrence NJ. Combretastatin-like chalcones as inhibitors of microtubule polymerisation. Part 2: Structure-based discovery of alpha-aryl chalcones. *Bioorg Med Chem.* 2009; 17:7711–7722.
39. Bhattacharyya B, Panda D, Gupta S, Banerjee M. Antimitotic activity of colchicine and the structural basis for its interaction with tubulin. *Med Res Rev.* 2008; 28:155–183.
40. Mahmoudian M, Rahimi-Moghaddam P. The anti-cancer activity of noscaptopine: a review. *Recent Pat Anticancer Drug Discov.* 2009; 4:92–97.
41. ClinicalTrials.gov. A Study of Noscaptopine HCl (CB3304) in Patients With Relapsed or Refractory Multiple Myeloma: <https://clinicaltrials.gov/ct2/show/record/NCT00912899>, (accessed September 23, 2015).
42. Barken I, Geller J, Rogosnitzky M. Prophylactic noscaptopine therapy inhibits human prostate cancer progression and metastasis in a mouse model. *Anticancer Res.* 2010; 30:399–401.
43. Zhou J, Liu M, Aneja R, Chandra R, Joshi HC. Enhancement of paclitaxel-induced microtubule stabilization, mitotic arrest, and apoptosis by the microtubule-targeting agent EM012. *Biochem Pharmacol.* 2004; 68:2435–2441.
44. Zhou J, Liu M, Luthra R, Jones J, Aneja R, Chandra R, Tekmal RR, Joshi HC. EM012, a microtubule-interfering agent, inhibits the progression of multidrug-resistant human ovarian cancer both in cultured cells and in athymic nude mice. *Cancer Chemother Pharmacol.* 2005; 55:461–465.

45. Mane JY, Semenchenko V, Perez-Pineiro R, Winter P, Wishart D, Tuszynski JA. Experimental and computational study of the interaction of novel colchicinoids with a recombinant human α / β I-tubulin heterodimer. *Chem Biol Drug Des.* 2013; 82:60–70.
46. Van de Weert M, Stella L. Fluorescence quenching and ligand binding: A critical discussion of a popular methodology. *J Mol Struct.* 2011; 998:144–150.
47. Lakowicz JR. *Principles of fluorescence spectroscopy.* New York: Kluwer Academic/Plenum. 1999
48. St.George M. *Drug Resistance in Breast Cancer: Characterization of Rationally Designed Paclitaxel Analogs in Model Systems.* University of Alberta; 2013.
49. Case DA, Babin V, Berryman JT, Betz RM, Cai Q, Cerutti DS, TE Cheatham III, Darden TA, Duke RE, Gohlke H, Goetz AW, Gusarov S, Homeyer N, et al. In *AMBER 2015;* University of California: San Francisco, 2015.
50. Chemical Computing Group Inc.: 1010 Sherbooke St. West, Suite #910, Montreal, QC, Canada, H3A 2R7, 2013.08.